which is in good agreement with observations. However due to lower *T* it might be reasonable to assume the first term in Eq. [1] to be lower (function of the activation energies for vaporization, usually in the order of 35-59 kcal/mol) and the second and third terms in Eq. [1] to have overcompensated for the observed losses. Accordingly, simple considerations call either for an increase in the exponent of the corrosion term and/or for an increase of the third term in Eq. [1]. However, as the increase of iR (Fig. 1) tends to exclude creepage, and because lithiation of the anode was not dramatic, we conclude that our main concern is the corrosion term, most likely in the form of wet seal corrosion (7). This conclusion is supported by noticing that in the interval up to 4000h the performance drop was in the order of 48 mV (*ca.* 12 mV/1000h) which include the observed iR increase and variations of the electrode potentials. This confirms that up to that time the performance of the electrodes was almost constant. On the other hand, the observed sharp drop in the performance (roughly 60 mV) after 4000h cannot be justified by the smaller increase of iR. This appears to demonstrate that the increase in the electrode overpotentials can be attributed to electrolyte loss.

Acknowledgments

Part of this work has been carried out under contract from the European Community (Non-nuclear Energy Program Contract no. EN3E-0068-I). SEM and XRD analysis have been made at CNR-IRTEC Faenza, Italy, through the assistance of Professor S. Galvagno of this Institute.

Manuscript submitted March 4, 1987; revised manuscript received Aug. 25, 1987. This was in part Paper 412 presented at the Boston, MA, Meeting of the Society, May 4-9, 1986.

CNR-Transformation and Storage of Energy assisted in meeting the publication costs of this article.

REFERENCES

1. B. Baker, S. Gionfriddo, A. Leonida, M. Maru, and P. Patel, Final Report for GRI Contract no. 5081-244-0545, Energy Research Corporation, Danbury, CT (1983).
2. S. Freni, R. Quagliata, F. Romeo, P. Carbonaro, and R. Di Leonardo, Internal Report no. 06/85 (April 1985).
3. N. Giordano, S. Freni, R. Quagliata, G. Moleti, P. Carbonaro, and E. H. Camara, in "Load Leveling and Energy Conservation in Industrial Processes," D.-T. Chin, Editor, p. 175, The Electrochemical Society Softbound Proceedings Series, Pennington, NJ (1986).
4. H. C. Maru, D. Patel, and L. Paetsch, Abstract 9, p. 27, The Electrochemical Society Extended Abstracts, Vol. 81-1, Minnneapolis, MN, May 10-15, 1981.
5. E. T. Ong and T. D. Clear, "Molten Carbonate Fuel Cell Technology," J. R. Selman and T. D. Clear, Editors, p. 54, The Electrochemical Society Softbound Proceedings Series, Pennington, NJ (1984).
6. L. G.Marianowski and J. B. O'Sullivan, Paper presented at the Eighth Annual Energy Technology Conference and Exposition, Washington, DC, March 9-11, 1981.
7. R. A. Donado, L. G. Marianowski, H. C. Maru, and J. R. Selman, *This Journal*, **131**, 2535, 2541 (1984).

Photodeposition of Ru on InP and GaInPAs

Catalytic and Electronic Properties

H. J. Lewerenz and R. Michaelis

Hahn-Meitner-Institut Berlin, Bereich Strahlenchemie, D-1000 Berlin 39, Germany

Photoassisted deposition of catalytically active transition metals on semiconductors has attracted considerable attention in recent years (1-4). Efficient photoelectrocatalysis cells producing H_2 with an efficiency well above 10% were based on such metal/semiconductor structures (1, 3, 5). Another approach involves semiconductor particle suspensions in which different transition metals are employed to run a presumably autocatalytical reaction leading to the splitting of water by light, for instance (6-8).

The functioning of these devices is being intensively investigated at present (9-11). It is meanwhile well established that exposure of transition metals to H_2 can result in pronounced work function changes (9, 10, 12-17). Hydrogen sensors employing MOS transistors are based on that principle (12, 13). The behavior of catalyst/semiconductor structures upon hydrogenation is not always easily correlated with the metal work function (10) and appears to merit further investigation on a selected system. We therefore restrict the present investigation to Ru/InP and Ru/GaInPAs contacts. The large grain polycrystalline quaternary semiconductor has been chosen because of differences in surface chemistry (18, 19). Polycrystalline Ru exhibits a work function very close to the normal hydrogen electrode, ϕ_{NHE} (20). On other metals hydrogenation was found to induce work function changes resulting in values corresponding to the standard potential of the NHE (3). Eventual changes in rectification behavior of semiconductor-hydrogenated Ru contacts are then unlikely to result from the metal work function changes upon hydrogenation.

Experimental

Electrochemical experimentation was done in the standard three-electrode potentiostatic arrangement using a potentiostat (HEKA) and a carbon counter- and a calomel reference electrode. Solutions were prepared from analytical grade chemicals and triple distilled water. For photodeposition, a W-I lamp (*ca.* 100 mW cm^{-2} intensity) was used. Metal deposition was done (*i*) from acidic $RuCl_3$ solution or (*ii*) from a ruthenium-nitridochloro complex compound exhibiting a higher Ru-deposition rate inferred from galvanic experiments (21). Substrate and deposit analysis with respect to photoactivity was performed by scanning laser spot analysis (SLS), uisng a He-Ne laser ($\lambda = 633$ nm) with spot size of 20 μm. Details will be given elsewhere (22).

Energy dispersive x-ray fluorescence (XRF) is performed with a commercial Tracor TN 5400 system with semiquantative element analysis. Characterization of the fundamental semiconductor properties of GaInPAs was done by photocurrent spectroscopy, XRF and C-V measurements (22). XRF revealed a composition of $Ga_xIn_{1-x}P_yAs_{1-y}$ with $x = 0.33$ and $y = 0.84$; for InP, the stoichiometry has been confirmed within 1 atmosphere percent accuracy. From Vegards law (23) and photocurrent spectroscopy, we obtain $E_g = 1.54$ eV and 1.46 eV for GaInPAs, respectively. The net acceptor concentration as determined by C-V measurements was $N_A\text{-}N_D = 3.2 \cdot 10^{17}\ cm^{-3}$ for InP and $1.5 \cdot 10^{18}\ cm^{-3}$ for $Ga_{0.33}In_{0.67}P_{0.84}As_{0.16}$, using $\epsilon = 12.3\ \epsilon_o$ calculated from Vegard's law (22-24).

Results

Figure 1 shows photocurrent-voltage curves for p-InP and p-$Ga_{0.33}In_{0.67}P_{0.84}As_{0.16}$ in 1*M* HCl with and without electrodeposited Ru catalyst. The data are compared with those from Pt metal. The figure shows that the typical current enhancement upon metallization is found. The increase in catalytic activity is larger for InP. A somewhat lower overall photoactivity is noted for GaInPAs.

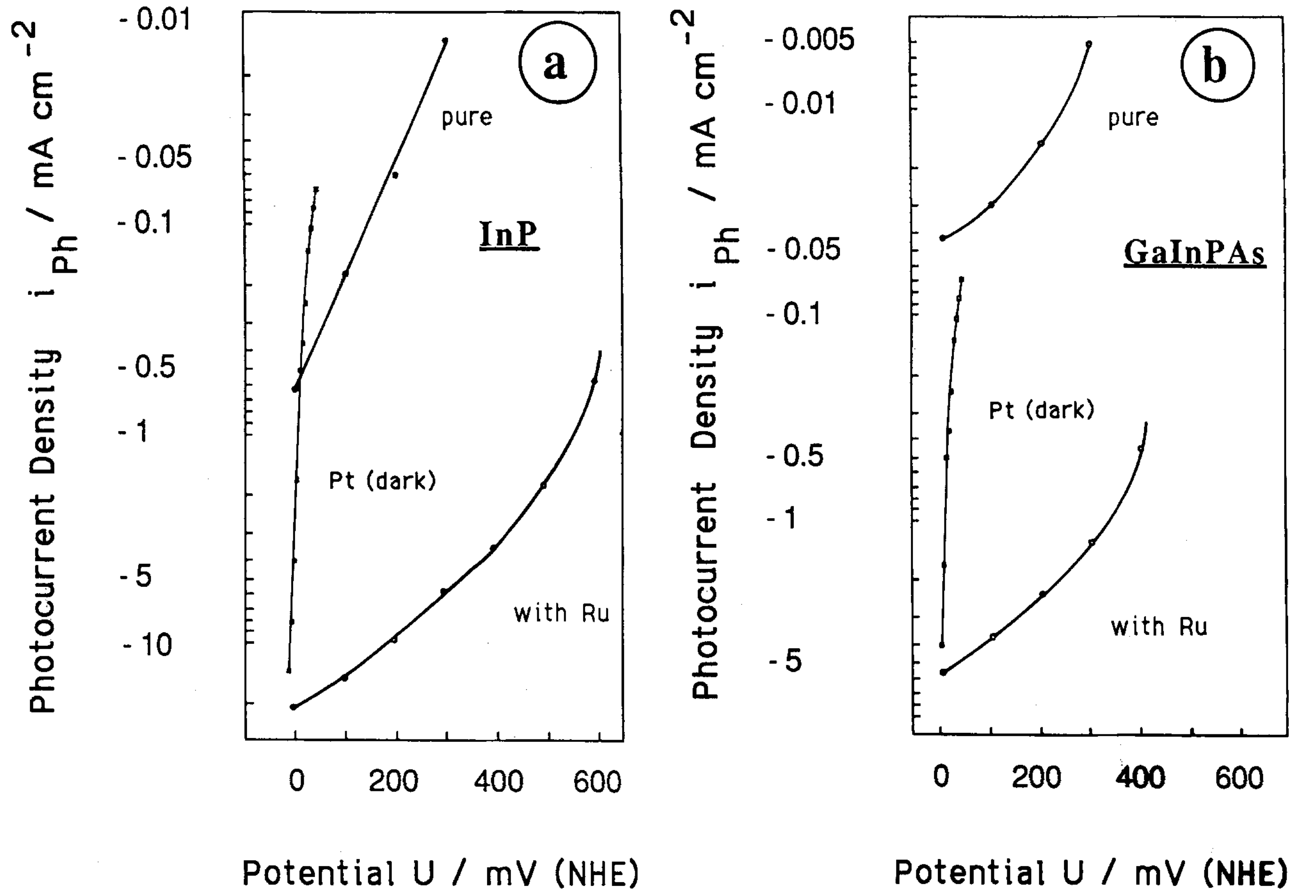

Fig. 1. Photocurrent-voltage characteristics of p-InP and p-GaInPAs before and after Ru deposition compared to the activity of Pt metal; solution, 1*M* HCl; light intensity, 300 mW cm^{-2}, W-I lamp; solution for Ru deposition, 0.06*M* $(NH_4)_3[Ru_2NCl_8(H_2O)_2]$-0.1*M* HCl, N_2 saturated; light intensity *I* for deposition 100 mW cm^{-2}; (a) p-InP, (b) p-$Ga_{0.33}In_{0.67}P_{0.84}As_{0.16}$.

Figure 2 shows scanning laser spot micrographs of Ru/p-InP and Ru/p-GaInPAs contacts. Differences in photoactivity are more pronounced on the polycrystalline GaInPAs photocathode. Accordingly the homogeneity of the Ru deposit is much less on GaInPAs compared to InP as evidenced by XRF (Fig. 3). Here the distribution of Ru metal across a p-GaInPAs sample after light assisted deposition is displayed. The left-hand side shows regions of approximately 20 μm width with high Ru signal (light areas) and similarly sized regions with low or very low Ru signal (dark areas). A typical line scan across such surface is shown on the right-hand side where strong variations of the Ru fluorescence signal with distance are found.

Figure 4 displays dark I-V characteristics obtained after metal deposition on p-GaInPAs. Before hydrogenation (curve 1), good rectifying behavior is observed. The calculated barrier height ϕ_B is obtained from

$$\phi_B = \frac{kT}{e} \ln \frac{A^{**}T^2}{I_S} \qquad [1]$$

where we have used the fact that the junction ideality factor is close to 1 determined from log *I* *vs.* *V*oc plots. Using $A^{**} = 64.8$ Acm^{-2}K^{-2}, a barrier height of $\phi_B = 0.74$V is obtained. H_2 evolution drastically changes the characteristic towards ohmic behavior (curve 2). Active vacuum pumping results in less rectification than before H_2 evolution according to curve 3. Increased H_2 evolution results in ohmic behavior (curve 4) and subsequent vacuum pumping (curve 5) results in less rectifying behavior than observed after treatment according to curve 2 (see curve 5). The effect of the hydrogen on the structure can obviously not fully be eliminated by extended high vacuum exposure.

Discussion

The I-V curves shown in Fig. 1 and compared to Pt metal characteristics are similar to the ones obtained on Rh/single-crystalline p-InP contacts (3). The fill factor for InP is somewhat less in our case which might either be due to differences in contact formation or due to the presence of a natural instead of an optimized intermediate oxide layer.

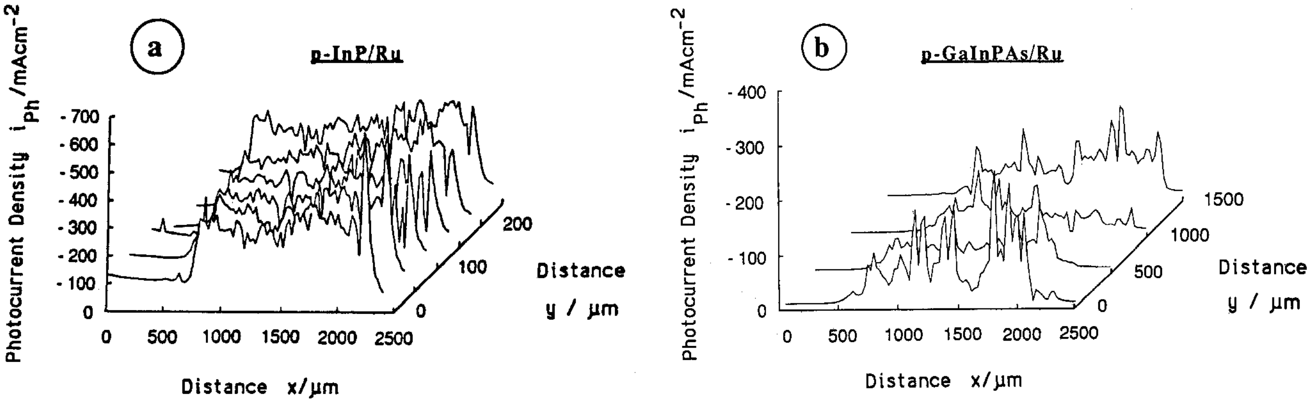

Fig. 2. Scanning laser spot analysis for (a) p-InP and (b) polycrystalline p-GaInPAs after Ru deposition; electrode potential −0.2V (SCE), He-Ne laser, *I*, 16W cm^{-2} at 20 μm spot size; solution, 0.1*M* HCl.

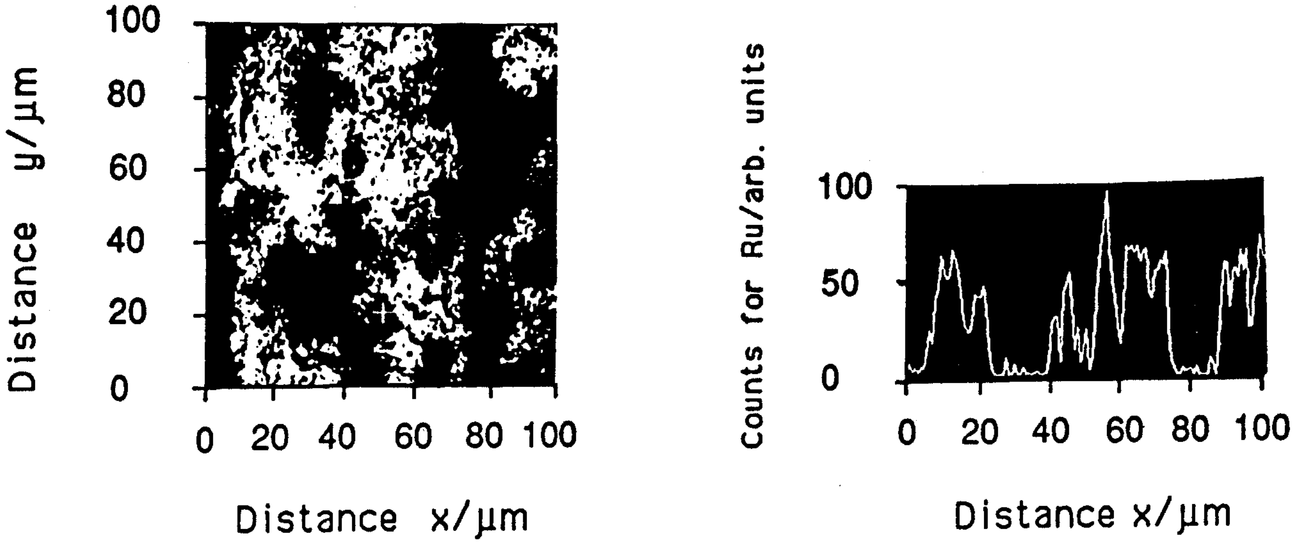

Fig. 3. X-ray fluorescence analysis of the Ru signal obtained from polycrystalline p-GaInPAs after metal deposition; contrast definition: high Ru count rate, light areas: low count rate, dark areas; the line scan shows variations of Ru-signal across selected regions of the sample; beam energy, 7 keV.

The photocurrent of the quaternary compound is smaller by a factor of ~ 10 compared to InP which can be attributed to the polycrystallinity of the GaInPAs samples or possibly to the increased recombination at relatively high doping levels. The photocurrent enhancement of Ru-plated InP over GaInPAs, however, is only ~3, indicating that local electrical fields and barriers at grain boundaries and imperfections of GaInPAs are partly compensated by the presence of the catalyst.

Nevertheless, the polycrystallinity reveals itself in the spatial dependence of the photocurrent (compare Fig. 2a and b). Therefore, the spatially integrated current measurement in Fig. 1 shows that the lower catalytic photocurrent on GaInPAs obviously results from different photoactivity of different grains. The photodeposition process is obviously more inhomogeneous on the polycrystalline samples. This is supported by the XRF microanalysis of Fig. 3 which evidences a considerable variation in Ru thickness across the sample. In particular the line scan shows drastic differences in Ru metal thickness. The correlation of catalyst metal thickness and photoactivity at different grains is described elsewhere (22). Generally, more information on the film morphology (microscopic porosity, island formation) is necessary. Since Schottky barrier formation occurs in the monolayer coverage range and below (25, 26), an increase in H_2 evolution rate due to increased Ru metal thickness appears unlikely, particularly with films of d ~ 200Å (22). A porous structure exhibiting a significantly enhanced active surface could account for the experimental observations.

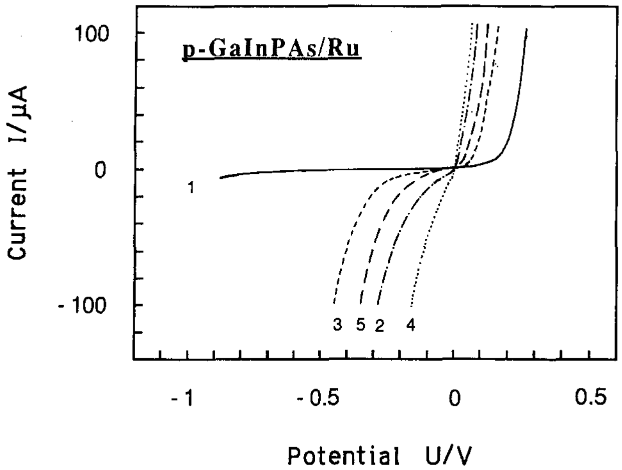

Fig. 4. Dark I-V characteristics of Ru/p-GaInPAs junctions; curve 1, before hydrogen evolution; curve 2, after H_2 evolution; Q, 3.5C; curve 3, after active vacuum pumping, 10^{-6} torr for 30 min; curve 4, after H_2 evolution, Q, 14C; curve 5, after active vacuum pumping.

The experimental result shown in Fig. 4 is at first glance in contradiction with earlier observations on InP (10). Instead of increased rectification, a transition to ohmic behavior is found on the quaternary compound. In simple terms this has to be achieved by an increase in metal work function or a decrease in semiconductor electron affinity or a combination of these changes. The relevant factors affecting the work function are surface/interface dipole layers, alloying, doping by hydrogen, and metal surface reconstruction.

In our experiment, hydrogen was evolved *in situ* which means that a large amount of atomic hydrogen is formed and adsorbed as precursor step to gas evolution. In this case the probability for hydrogen atoms to diffuse to the metal-semiconductor interface is high. Also, the presence of residual oxygen known to block hydrogen insertion, as postulated in gas phase experiments to explain the barrier height increase on p-InP/Ru contacts upon hydrogen exposure (10), is not likely under our strongly reducing conditions. The hydrogen adsorption at the semiconductor surface can result in a drastic reduction of semiconductor electron affinity due to the dipole formed. The influence of hydrogen alloying is obviously small (9) and the metal/ambient interface has been investigated to some extent by surface analytical methods (27-31). The results show that changes in the 0.1 eV range are observed. Increases as well as lowering of the work function has been found and is attributed to different (r and s) adsorption sites (32). S-type adsorption sites are described as hydrogen adsorption (hydrogen atoms below the geometrical surface plane) whereas r-type adsorption corresponds to hydrogen on top of the metal. We believe this effect to be of minor importance here. Of greater effect appears to be the dipole formation at the semiconductor surface.

In this case, the different behavior of p-InP/Ru must be explained. There are two distinctions to be made:

1. The absolute amount of dissociated hydrogen, when supplied from the gas phase is probably considerably lower than in case of *in situ* H_2 evolution. In addition, the presence of oxygen has been postulated on gas exposed catalyst surfaces (10). It is also known that oxygen acts as a blocking factor to insertion of hydrogen (35). It therefore appears reasonable to assume a reduced amount of dissolved hydrogen within the catalyst. Hence the formation of a dipole layer at the metal/semiconductor interface might be suppressed to some extent.

2. In addition, on InP and particularly on the (111) face, an oxide film of tunnel thickness is always present (19, 33, 34). Experiments on Pd-Si MOS transistors used as hydrogen sensors have evidenced that hydrogen does not

penetrate the oxide. It appears therefore probable that in addition to reduced supply of atomic hydrogen, dipole layer formation at the InP surface is inhibited.

3. The surface chemistry on GaInPAs is quite different. Work on passivation phenomena on III-V compounds shows that stable oxides are not formed on GaAs, for instance (18). Energy dispersive x-ray fluorescence analysis reveals a homogeneous distribution of the elemental constituents of the quaternary compounds; hence the surface will exhibit Ga and As atoms corresponding to the stoichiometry. It appears reasonable to assume that the absence of a compact oxidic layer on the quaternary compound allows penetration of hydrogen, produced during H_2 evolution, possibly along grain boundaries to the semiconductor surface, resulting in a pronounced electron affinity change. This view is supported by the behavior of the contacts after hydrogenation and vacuum pumping (curves 3 and 5 in Fig. 4). Since the original rectifying behavior cannot be attained after vacuum pumping, some hydrogen must be bound within the structure. If hydrogen is adsorbed at the semiconductor surface in different sites (removable and permanent hydrogen), increased ohmic behavior should result in less rectifying properties after vacuum pumping. This is indeed observed in Fig. 4 (compare curves 2, 3 and 4, 5).

4. Another possibility which has not been discussed so far could be a work function increase of Ru during hydrogen evolution. More densely packed Ru single-crystal surfaces exhibit a vacuum work function of approximately 5.2 eV, *i.e.*, 0.5 eV higher than on evaporated polycrystalline films (36). Information on metal surface reconstruction due to H_2 gas evolution, however, is not available at present. Therefore, suggestion (no. 4) is highly speculative.

Regarding the information in the literature, the most likely explanation is as given in (no. 2) and (no. 3), possibly some influence of the effects discussed in (no. 1) do also contribute to the differences with respect to the Ru/InP system. We summarize by stating that the differences in surface chemistry, particularly in oxide formation in conjunction with a high generation rate of atomic hydrogen can qualitatively explain our results. The feasibility of hydrogen sensors with Ru is limited to systems where hydrogen would adsorb reversibly at the semiconductor surface. This has not been observed in our case.

Acknowledgments

The authors thank Professor K. J. Bachmann and F. A. Thiel for growing the quaternary compound and K.-D. Husemann for assistance in the diode and microprobe analysis experiments. Dr. A. Werner was involved in the preliminary stage of experimentation. Valuable discussions with Professor H. Tributsch, Professor D. Schersson, and Dr. G. Betz are gratefully acknowledged.

Manuscript submitted Feb. 25, 1987; revised manuscript received Sept. 2, 1987.

REFERENCES

1. A. Heller and R. G. Vadimsky, *Phys. Rev. Lett.*, **46,** 1153 (1981).
2. C. Levy-Clement, A. Heller, W. A. Bonner, and B. A. Parkinson, *This Journal*, **129,** 1701 (1982).
3. A. Heller, E. Aharon-Shalom, W. A. Bonner, and B. Miller, *J. Am. Chem. Soc.*, **104,** 6942 (1982).
4. A. Heller, *Science*, **223,** 1141 (1983).
5. E. Aharon-Shalom and A. Heller, *This Journal*, **129,** 2865 (1982).
6. E. Borgarello, K. Kalyanasundaram, M. Grätzel, and E. Pelizetti, *Helv. Chim. Acta*, **65,** 243 (1982).
7. M. Grätzel, in "Photochemical Conversion and Storage of Solar Energy," J. S. Connolly, Editor, Academic Press, Inc., New York (1981).
8. A. Henglein, *Ber. Bunsenges. Phys. Chem.*, **86,** 241 (1982).
9. D. E. Aspnes and A. Heller, *J. Vac. Sci. Technol.*, **B1,** 602 (1983).
10. D. E. Aspnes and A. Heller, *J. Phys. Chem.*, **87,** 4919 (1983).
11. M. Schindler, M. Kunst, and H. Tributsch, To be published.
12. K. I. Lundström, M. S. Shivaraman, and C. M. Svensson, *J. Appl. Phys.*, **46,** 3876 (1975).
13. I. Lundström, M. S. Shivaraman, C. M. Svensson, and L. Lundkrist, *Appl. Phys. Lett.*, **26,** 55 (1975).
14. I. Lundström, M. S. Shivaraman, and C. M. Svensson, *Surf. Sci.*, **64,** 497 (1977).
15. K. Ito, *ibid.*, **86,** 345 (1979).
16. N. Yamamoto, S. Tonomura, T. Matsuoka, and H. Tsubomura, *ibid.*, **92,** 400 (1980).
17. N. Yamamoto, S. Tonomura, T. Matsuoka, and H. Tsubomura, *J. Appl. Phys.*, **52,** 6227 (1981).
18. S. Menezes, B. Miller, and K. J. Bachmann, *J. Vac. Sci. Technol.*, **B1,** 48 (1983).
19. H. J. Lewerenz, D. E. Aspnes, B. Miller, D. L. Malm, and A. Heller, *J. Am. Chem. Soc.*, **104,** 3325 (1982).
20. R. Gomer and G. J. Tryson, *J. Phys. Chem.*, **66,** 4413 (1977).
21. G. S. Reddy and P. Taimsalu, *Trans. Inst. Metal Finish*, **47,** 187 (1969).
22. R. Michaelis, H. J. Lewerenz, and K.-D. Husemann, To be published.
23. R. E. Nahory, *Appl. Phys. Lett.*, **33,** 659 (1978).
24. K. Nakajima, *J. Appl. Phys.*, **49,** 5944 (1979).
25. R. H. Williams, A. McKinley, G. J. Hughes, V. Montgomery, and I. T. McGovern, *J. Vac. Sci. Technol.*, **21,** 594 (1982).
26. I. T. McGovern and J. F. McGilp, *Vacuum*, **33,** 607 (1983).
27. K. Krämer and D. Menzel, *Ber. Bunsenges. Phys. Chem.*, **78,** 728 (1974).
28. L. R. Danielson, M. J. Dresser, E. E. Donaldson, and J. T. Dickinson, *Surf. Sci.*, **71,** 599 (1978).
29. J. A. Schwarz, *ibid.*, **87,** 525 (1979).
30. H. Shimizu, K. Christmann, and G. Ertl, *J. Catal.*, **61,** 412 (1980).
31. P. Feulner and D. Menzel, *Surf. Sci.*, **154,** 465 (1985).
32. J. Horiuti and T. Toya, in "Solid State Surface Science," Vol. 1, M. Green, Editor, Marcel Dekker, Inc., New York (1969).
33. A. Heller, B. Miller, H. J. Lewerenz, and K. J. Bachmann, *J. Am. Chem. Soc.*, **102,** 6556 (1980).
34. S. Menezes, H. J. Lewerenz, F. A. Thiel, and K. J. Bachmann, *Appl. Phys. Lett.*, **38,** 710 (1981).
35. J. Hrbek, *J. Phys. Chem.*, **90,** 6217 (1986).
36. Christmann (et al.), to be published